Chemical Science

Accepted Manuscript

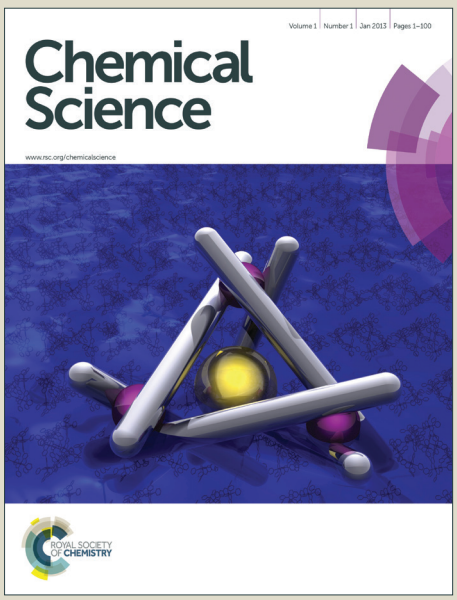

ROYAL SOCIETY OF CHEMISTRY

www.rsc.org/chemicalscience

Journal Name

RSCPublishing

ARTICLE

Top-Down Strategies for the Structural Elucidation of Intact Gram-negative Bacterial Endotoxins

Cite this: DOI: 10.1039/x0xx00000x

John P. O'Brien,[a] Brittany D. Needham,[b] Dusty B. Brown,[b] M. Stephen Trent, [b] and Jennifer S. Brodbelt[a] *

Received 00th January 2012,
Accepted 00th January 2012

DOI: 10.1039/x0xx00000x

www.rsc.org/

Re-modelling of lipopolysaccharides, which are the primary constituent of the outer cell membrane of Gram-negative bacteria, modulates pathogenesis and resistance to microbials. Reported herein is the characterization of intact Gram-negative bacterial lipooligosaccharides (LOS) via a new strategy utilizing online liquid chromatography (LC) coupled with ultraviolet photodissociation (UVPD) mass spectrometry. Compared to collision-based MS/MS methods, UVPD and UVPD/HCD promoted a greater array of cleavages within both the glycan and lipid moieties, including C-C, C-N, C-O cleavages in the acyl chains as well as glycosidic and cross-ring cleavages, thus providing the most far-reaching structural characterization of LOS. This LC-MS/MS strategy affords a robust analytical method to structurally characterize complex mixtures of bacterial endotoxins that maintains the integrity of the core oligosaccharide and lipid A domains of LOS, providing direct feedback about the cell envelope architectures and LOS modification strategies involved in resistance host innate immune defense.

Introduction

Lipopolysaccharides (LPS) are the chief component of the outer cell membrane of Gram-negative bacteria and play a key role in the innate immune response during pathogenic invasion.[1–4] In general, LPS possesses a complex structural architecture comprised of a hydrophobic glycolipid domain (called lipid A) and a hydrophilic polysaccharide chain containing a core oligosaccharide and a distal O-antigen polysaccharide tail (**Figure 1**). Some bacteria possess LPS lacking the O-antigen; these LPS are alternatively called rough LPS (R-LPS) or lipooligosaccharides (LOS). Breakdown of the cell membrane releases LPS which creates a potent immunological response via the recognition of the lipid A moiety by the mammalian microbial recognition receptor, Toll-like receptor 4 (TLR4).[4] This event triggers a signaling cascade that promotes the production of pro-inflammatory cytokines; the net outcome can either lead to beneficial bacterial clearing or may cause the potentially deadly hyper-immune response known as endotoxic shock.[4] For many mucosal pathogens including *Haemophilus influenza*, *Campylobacter jejuni*, and pathogenic *Neisseria*, dynamic structural variation of the LOS plays a key role in bacterial infection and human disease.

Structural remodeling of LPS/LOS facilitates Gram-negative pathogenesis in various capacities, such as evasion of host defense systems, and resistance to antimicrobials. Due to limited methods for structural analysis of intact LPS/LOS, much of the progress in understanding LPS/LOS modifications has focused on lipid A.[1,3] Lipid A synthesis is largely conserved among Gram-negative bacteria, but it is now established that lipid A post-synthetic modifications are diverse and frequent among bacteria.[1,3] Many lipid A modifications are adaptations

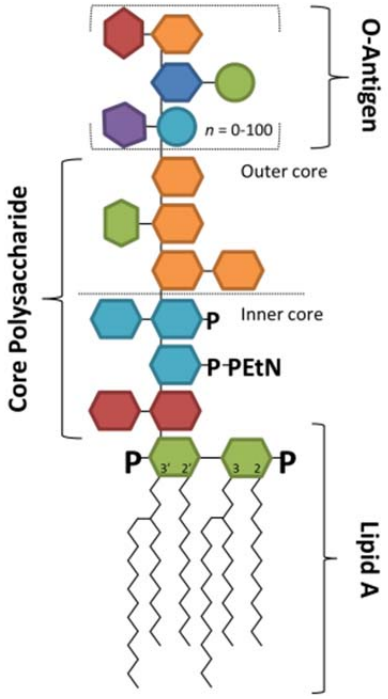

Figure 1. Structural diagram showing the lipid A, core polysaccharide and O-antigen components of lipopolysaccharides. Lipooligosaccharides (LOS) are lipopolysaccharides containing only core polysaccharides and the lipid A anchor.

to enhance resistance to cationic antimicrobial peptides (CAMPs) and modulate their detection from the host TLR4-myeloid differentiation factor 2 (TLR4-MD2) immune receptor.[1,3,5] CAMPs, such as host defensins and polymyxin antibiotics, are a class of positively charged amphipathic peptides that attach to the negatively charged bacterial surface and embed into the membrane, disrupting membrane stability and cellular function.[6] Cationic modifications of the lipid A with the addition of aminoarabinose, glycine or phosphoethanolamine moieties limit the interaction between lipid A and CAMPs and afford CAMP resistance.[3,7] Other important lipid A modifications including changes in the number and location of the acyl chains, variations of the phosphorylation pattern, and hydroxylation of the acyl chains have been implicated in the down regulation of the TLR-4 response.[8] However, connections between lipid A modification and the nature of the oligosaccharide attached to particular lipid A moieties are lost when using analytical methods that entail hydrolysis prior to structural analysis, a common practice adopted in many conventional workflows.

The LPS core and O-antigen regions vary not only between species but also among strains of the same species. For example, *E. coli* has five known core structures and many different O-antigen regions, both of which can be further modified in response to various environmental stresses.[4] Several reports demonstrate that various chemical groups, such as additional sugars, and phospho-form groups like phosphate, phosphoethanolamine and phosphorylcholine can be transferred onto the LPS core regions giving rise to immunological diversity.[3,4] Similarly, O-antigen can be customized through glycosylation,[9] acetylation,[10] addition of phosphoryl constituents,[4] and ligation of acidic repeats such as colonic[11] and sialic acids.[12] Such modifications have historically been difficult to characterize, yet they play important roles in bacterial survival within a host and affect the treatment of infectious disease. The improved analysis of core and O-antigen modifications could also accelerate vaccine development for organisms for which the LPS on the bacterial surface is a major protective antigen.[13] Until now, conserved epitopes in the LOS/LPS among certain pathogenic bacteria have been difficult to identify due to the natural heterogeneity within each strain and diverse core modifications each employs. Thus, there is an underlying need to develop robust methods for identifying and characterizing intact LPS and LOS that cover the gram-negative bacterial surface.

Mass spectrometry over the past two decades has been adopted as the standard method for lipid A and LPS structural analysis.[14-19] Mass analysis of intact LOS has largely been performed using MALDI-MS[14–18] due to the underlying solubility issues of LOS which have inhibited efficient ionization by ESI. In fact, few studies have reported the characterization of intact LPS and LOS by mass spectrometry,[14–22] and instead the LPS are chemically treated to partition lipid A species and oligosaccharides that are subsequently analyzed by tandem mass spectrometry.[23,24,5,25–41] This latter approach typically relies on mild acid or alkaline hydrolysis or hydrazine treatment to deacylate the lipid A moieties or to remove the glycan chains.[42] This work-around is problematic because hydrolysis degrades acid and base labile modifications such as the phosphoethanolamine, diphosphate, aminoarabinose or acetate groups and eliminates important structural information from analysis.

Once the lipid A or polysaccharide groups are isolated, they are typically analyzed via tandem mass spectrometry (MS/MS) to generate diagnostic fragmentation patterns to characterize the structures. Collision induced dissociation (CID)[5,17,22–40] and infrared multiphoton dissociation (IRMPD)[29,41] have been utilized to elucidate lipid A structure. CID in particular is the benchmark method MS/MS method for elucidation of lipid A structures, but several stages of sequential ion activation are frequently required to adequately characterize the complex structures. There still remain many challenges for the structural characterization of intact LOS. As a promising alternative, UVPD is a higher energy activation method that has demonstrated advantages over CID for characterization of a wide range of biopolymers (including lipids, proteins, peptides, nucleic acids, and glycans).[41,43–66] Hybrid activation methods consisting of UVPD in conjunction with CID or electron transfer dissociation (ETD) have also been developed as a means to yield even richer fragmentation patterns.[44,46] We have explored UVPD at 193 nm for characterization of glycolipids, including lipid A, and found that UV photoexcitation promotes extensive C-C, C-N, C-O, glycosidic and cross-ring cleavages which contribute to the highly informative fragmentation patterns observed upon UVPD.[41,61–66] UVPD has allowed unusual modifications to be accurately pinpointed and isobaric species to be differentiated.[41,61–66]

The development of better ionization and MS/MS strategies has advanced the characterization of lipid A and to a lesser extent LOS, but analysis of complex mixtures affords yet another hurdle. LPS and LOS exhibit an exceptional level of structural heterogeneity, a factor that can inhibit the detection of low abundance but immunologically relevant species using offline MS/MS methods and makes separation of confounding isobaric components essential. Chromatographic methods offer the best option for analysis of complex mixtures of bioanalytes, although successful implementation for LPS remains non-trivial.[72-82] Many of the separation methods, just like the mass spectrometric analytical methods, have relied on acid hydrolysis of the lipid A and the glycan moieties, a feature which makes it difficult to match the polysaccharide portions to the corresponding lipid A anchors for bacterial species that contain heterogeneous mixtures of up to several dozen different inner-core LPS types. Several HPLC-based methods have reported using ion pairing-based reversed phase separations for the analysis of LPS and LOS polysaccharides,[67–71] but there is yet to be a HPLC-MS method to analyze intact LPS and LOS without incorporating supplemental and potentially degrading derivatization techniques.[6]

Here we report the development of UVPD-MS and a hybrid MS/MS technique termed UVPD/HCD to characterize intact LOS using an Orbitrap mass spectrometer. We compare the UVPD methods to conventional CID and HCD for analysis of LOS from various mutants of *E. coli*. The photoactivation MS/MS strategy provides a diverse array of fragments to characterize both the lipid A and core moieties within an intact lipooligosaccharides. We also report the successful LC-MS analysis of intact, underivatized lipooligosaccharides that allows both qualitative and quantitative characterization of LOS mixtures while minimizing sample preparation artifacts. The simultaneous analysis of the LOS core and lipid A modifications provides insight into LPS/LOS global cellular architectures, a direct reflection of the immunogenicity and barrier capability of the outer membrane.

Experimental

Lipooligosaccharides and Solvents

Kdo_2-lipid A (*waaCwaaF*) LOS was purchased from Avanti Polar Lipids, Inc. (Alabaster, AL). LOS from the *E. coli* (K12 strain) BN1 and *waaQwaaG* mutants of strain BN1 (BN1 Δ*waaQwaaG*) was isolated from cultured cells using the hot water phenol extraction method as previously described.[8] Solvents for HPLC-MS and direct infusion were purchased from Sigma Aldrich, (St. Louis, MO).

Mass Spectrometry

All mass spectrometry and LC-MS experiments were performed using a Thermo Scientific Orbitrap Elite mass spectrometer (Bremen, Germany) modified to perform ultraviolet photodissociation (UVPD) using a recently described set-up.[72] All MS experiments were infused using the instrument's electrospray (ESI) source with a voltage set to 4 kV. Direct infusion experiments were performed using 5 μM LOS solutions in 50:50 chloroform:methanol at a flow rate of 3 μL/min. All UVPD experiments were performed using a Coherent ExiStar XS ArF excimer laser (Santa Clara, CA) producing 5 ns, 6 mJ pulses at 193 nm at a pulse repetition rate of 500 Hz. For all experiments, ten pulses were used. Due to the high divergence of the laser and lack of focusing/collimating optics, it is estimated that less than 1% of the beam enters the HCD cell. Higher collision energy dissociation (HCD) experiments were typically performed using a normalized collisional energy of 40% and a 0.1 ms activation time. For CID experiments, precursor ions were typically activated for 10 ms in the high pressure cell of the dual linear ion trap using a NCE energy of 25% and detected in the Orbitrap mass spectrometer. Hybrid HCD/UVPD was performed by simultaneously activating ions in the HCD cell at a HCD energy of 40% NCE along with simultaneous exposure of the ions to ten laser pulses. CID experiments were performed using the default isolation *q* value of 0.25. All MS/MS experiments were performed using a precursor isolation width of 3 m/z.

Liquid Chromatography

LOS separations were performed using a Dionex Ultimate 3000 microbore liquid chromatography system (Sunnyvale, CA). Approximately 1 microgram of sample was directly injected onto a XBridge C8 column from Waters (3 mm x 100 mm, 3.5 micron particles) column. After LOS was injected onto the column. Mobile phase A consisted of 50:50 methanol:water with 0.05% NH_4OH and mobile phase B consisted of 40:40:20 isopropyl alcohol:chloroform:methanol with 0.05% NH_4OH. Separations were performed using a 25 minute linear gradient at a flow rate of 300 μL/min starting at 15% mobile phase B to 70% mobile phase B before holding at 70% mobile phase B for 5 minutes and re-equilibrating for 5 minutes at 15% mobile phase B. ESI survey mass spectra were collected using a m/z range of 700-2000 and MS/MS experiments were performed as described above.

Results and Discussion

Analysis of intact *E. coli* LOS were undertaken using both direct infusion and HPLC-based strategies in conjunction with CID, HCD, UVPD and a new hybrid activation technique described here termed UVPD/HCD. These methods were compared using wild type BN1 and BN1 mutant LOS from *E. coli.* As reported for lipid A molecules,[41,61–66] UVPD of LOS results in a diverse array of fragmentation pathways for which there is no simple nomenclature or shorthand notation (as commonly used for the fragmentation of peptides, oligosaccharides and nucleic acids). Thus, the very rich MS/MS spectra upon UVPD are conveyed as fragmentation maps which display the bond cleavages (and sets of cooperative cleavages) that are consistent with the *m/z* values of the resulting product ions. Briefly, cleavage sites are numbered on the structures of each LOS and the fragment ions arising from those cleavages are listed next to numbered cleavage sites. Each MS/MS spectrum is accompanied by a fragmentation map.

Figure 2, which shows the MS/MS spectra of deprotonated

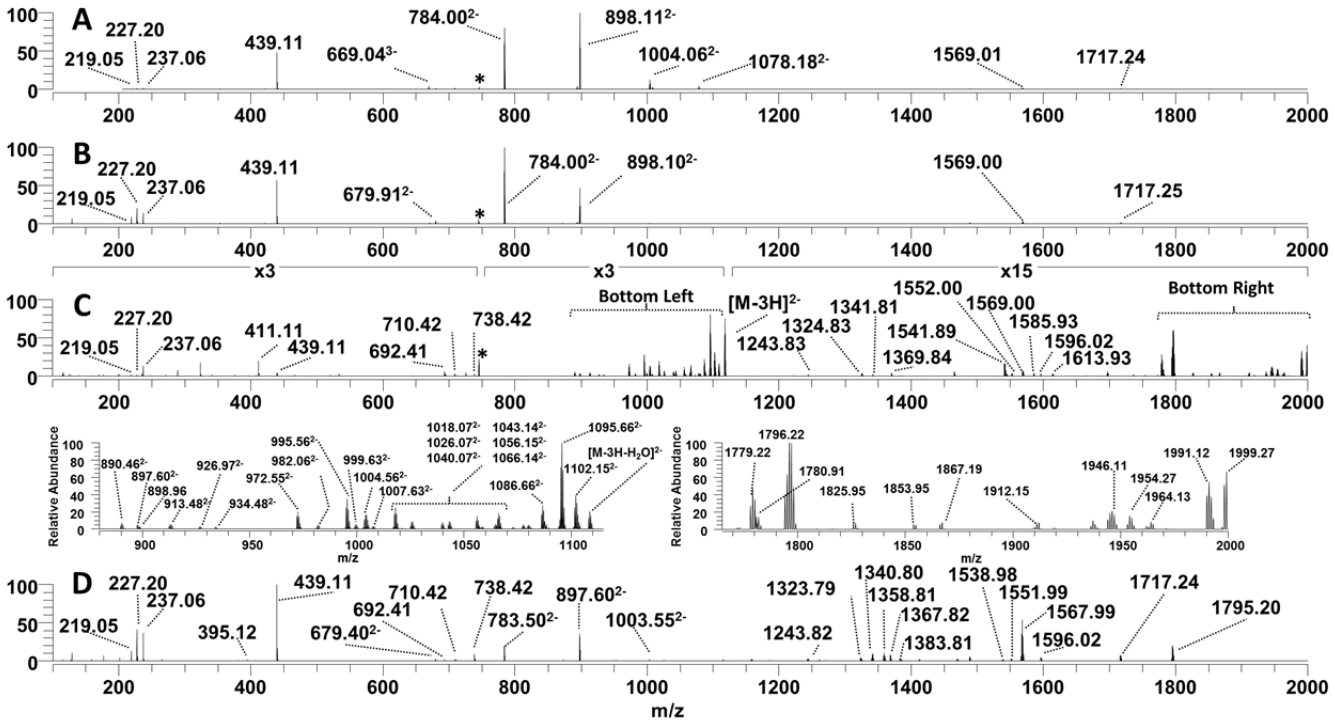

Figure 2. Tandem mass spectra of the triply deprotonated Kdo2-lipid A [Mr = 2237.34] (A) CID, (B) HCD, (C) UVPD and (D) UVPD/HCD. Zoomed in regions between m/z 880-1115 and m/z 1765-2000, respectively, are displayed below the UVPD spectrum. Fragmentation maps of Kdo2-lipid A and the fragment ions associated with each of the ion activation methods are shown in Figure 3.

Kdo_2-lipid A (z = 3−), is distilled to the series of fragmentation maps in **Figure 3** and **Table S1.** For this lipid, one key glycosidic cleavage that occurs between lipid A and the Kdo_2 disaccharide is labelled as site (3), and a number of the fragment ions observed in **Figure 2** are consistent with cleavage at site (3) (which may occur in conjunction with additional cleavages). The products which directly correspond to the resulting lipid A and Kdo sugar moieties are observed as ions of m/z 898.11 (z = 2−) and 439.11 (z = 1−) (like the ones seen in the CID spectrum in **Figure 2A**), but in some cases there are other related fragment ions that arise from multiple cleavage sites. For example, the fragment ion of m/z 784.00 (z = 2−) in **Figure 2A** is attributed to the same glycosidic cleavage (3) in addition to the loss of the myristoyl chain via cleavage site (5) in **Figure 3**. Therefore, the ion of m/z 784.00 (z = 2−) is affiliated with cleavage sites (3) and (5) in the fragmentation map. The fragmentation maps provide a convenient way to show the scope of cleavages that occur for the complex LOS molecules, ranging from simple phosphate and acyl chain losses to more elaborate pathways such as cross ring and carbon-carbon bond cleavages which are unique to UVPD.

MS/MS activation of *E. coli* Kdo2-Lipid A

Kdo_2-lipid A is a truncated LOS produced by a K12 *E. coli* mutant strain which lacks functional heptosyl transferases WaaC and WaaF that prevent further elongation of LOS sugars. Kdo_2-lipid A is frequently used in biological testing due to its significant activation of the TLR4 receptor. This glycolipid consists of two acidic Kdo (3-deoxy-D-manno-oct-2-ulosonic acid) sugars which are linked to the lipid A via a glycosidic bond at the 6'-glucosamine (GlcN) carbon. The lipid A anchor consists of two glucosamine sugars with phosphate groups at the 1 and 4' carbons and a total of four hydroxymyristoyl chains at the 2, 3, 2' and 3' positions via amide and ester bond linkages. The 2' and 3' acyl chains are further modified with lauristoyl and myristoyl secondary chains, respectively. The CID, HCD, UVPD and UVPD/HCD mass spectra of deprotonated Kdo_2-lipid A (z = 3−) are shown in **Figure 2,** and the corresponding MS/MS fragmentation maps of the spectra are displayed in **Figure 3**. Collisional activation of Kdo_2-lipid A, either by conventional low energy CID or by beam-type HCD, primarily promoted the C-O glycosidic cleavage between Kdo_2 sugars and lipid A (cleavage site (3)) as evidenced by the dominant fragment ions of *m/z* 439.11 (z = 1−) and 898.11 (z = 2−) which agrees with previous reports using CID.[73] Additionally, secondary cleavages associated with the loss of the myristoyl acyl chain (cleavage site (5)) in conjunction with (3) are consistent the fragment ions of *m/z* 784.00 (z = 2−) and 1359.01 (z = 1−). A product ion of *m/z* 1717.24 (z = 1−) is consistent with cleavage at site (3) along with the loss of a phosphate group. The products of *m/z* 669.04 (z = 3−) and 1004.06 (z = 2−) correspond to cleavage site (5), loss of the neutral or charged myristoyl fatty acid group. The CID and HCD fragmentation patterns of Kdo_2-lipid A are very similar, with both providing only a very limited number of fragment ion types that provide relatively little confirmatory information

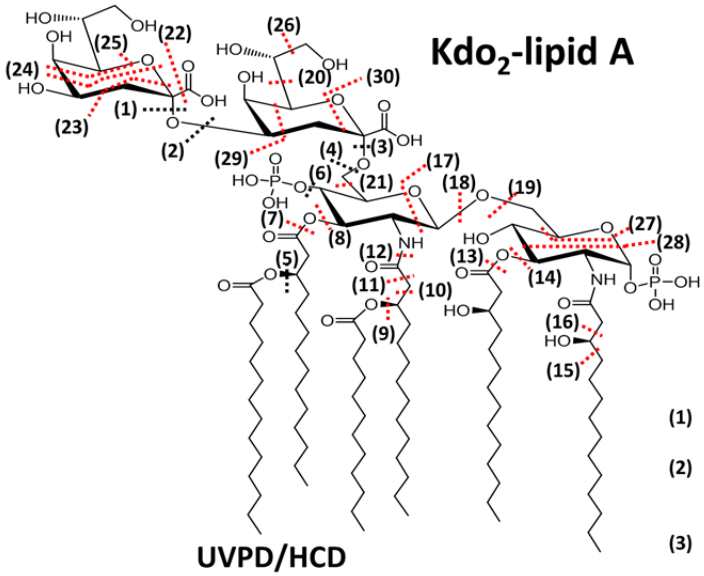

CID

(1) 219.05
(2) 237.06
(3) 439.11, 784.00^{2-}, 898.11^{2-}, 1569.01, 1717.24
(5) 227.20, 784.00^{2-}, 669.04^{3-}, 1004.06^{2-}
(6) 1078.18^{2-}, 1717.24

HCD

(1) 219.05
(2) 237.06
(3) 439.11, 679.91^{2-}, 784.00^{2-}, 898.10^{2-}, 1569.00, 1717.25
(5) 227.20, 784.00^{2-}
(6) 1717.24

UVPD/HCD

(1) 219.05
(2) 237.06
(3) 439.11, 679.40^{2-}, 783.50^{2-}, 897.60^{2-}, 1243.82, 1340.80, 1358.81, 1383.81, 1551.99, 1567.99, 1596.02, 1717.24
(4) 395.12, 1323.79, 1367.81
(5) 227.20, 783.50^{2-}, 1003.55^{2-}, 1567.99, 1358.81
(6) 1243.82, 1717.24
(8) 1243.82, 1323.79, 1340.80
(9) 1596.02
(12) 1367.82, 1383.81
(13) 1538.98
(14) 1551.99
(17) 738.42
(18) 710.42
(19) 692.41
(20) 395.12
(21) 1538.98

UVPD

(1) 219.05 (B_1), 1007.63^{2-} (Y_3)
(2) 237.06 (C_1), 999.63^{2-} (Z_3), 1999.27 (Z_3)
(3) 411.11, 439.11 (B_2), 897.60^{2-} (Y_2), 1243.82, 1341.81, 1551.99, 1569.00, 1596.02, 1796.22
(4) 395.12, 1324.83, 1369.84, 1779.22
(5) 227.20, 1004.56^{2-}, 1569.00
(6) 1243.82, 1717.24
(7) 898.96^{2-}
(8) 890.46^{2-}, 1243.82, 1324.83, 1341.81, 1780.91
(9) 1018.07^{2-}, 1596.02
(10) 934.48^{2-}
(11) 926.97^{2-}, 1853.95
(12) 913.48^{2-}, 1369.84, 1825.95
(13) 982.06^{2-}, 1538.98, 1964.13,
(14) 972.55^{2-}, 995.56^{2-}, 1551.99, 1946.11, 1991.12
(15) 1040.07^{2-}
(16) 1026.07^{2-}
(17) 738.42 ($^{1,5}X_1$)
(18) 710.42 (Y_1)
(19) 692.41 (Z_1), 1541.89 (C_3)
(20) 395.12, 411.11, 1086.66^{2-}
(21) 1538.98
(22) 972.55^{2-}, 982.06^{2-}, 1095.66^{2-}, 1946.11^{-}, 1964.13,
(23) 1043.14^{2-} ($^{0,2}X_3$)
(24) 1056.15^{2-} ($^{0,3}X_3$)
(25) 1066.14^{2-} ($^{3,5}X_3$)
(26) 1105.15^{2-}
(27) 1585.93 ($^{0,4}A_4$)
(28) 1613.93 ($^{0,3}A_4$)
(29) 1954.27 ($^{2,4}X_2$)
(30) 1867.19 ($^{1,5}X_2$)

Figure 3. MS/MS fragmentation maps of the LOS Kdo_2-lipid A [M_r=2237.34] using CID, HCD, UVPD/HCD, and UVPD. Cleavages specific to UVPD or UVPD/HCD are shown in red.

about the other acyl chains or nature of the attached sugar groups. UVPD resulted in a much richer fragmentation pattern, as illustrated for Kdo_2–lipid A in **Figure 2C** as well as the fragmentation map in **Figure 3**. Two of the more congested regions of the UVPD mass spectrum are expanded below **Figure 2C** (m/z 880 to 1110 and m/z 1770 to 2000) to illustrate that the fragment ions are resolvable with good signal-to-noise, allowing the assignment of accurate masses. UVPD generated a number of complementary fragment ion pairs (B/Y, C/Z) and cross ring cleavages (A/X) ions which are useful for the elucidation of the polysaccharide composition as well as the assignment of their branching patterns. The glycosidic and cross ring cleavages are enumerated as cleavage sites (16), (17) and (18). In addition diagnostic C-O and C-N cleavages associated with sites (6), (7), (11), (12) and (13) result in other key fragment ions upon UVPD which help map the set of acyl chains attached to the lipid A molecule (although not revealing the specific location of each chain). Moreover, several C-C bond cleavages (9), (10), (12), and (15) were uniquely observed upon UVPD and are crucial for identification of the absence or presence of acyl chain modifications that confer CAMP resistance (as noted upon UVPD of lipid A molecules).[62]

Although UVPD provides the greatest array of fragment ions, it also leads to electron photodetachment which produces the notable product ion labelled as [M – 3H] (z = 2−) (m/z 1117.6) in **Figure 2C**. In essence, UV photoabsorption promotes charge reduction of the selected precursor ion via detachment of an electron, resulting in an intact radical-type species. Because this pathway is uninformative, the UVPD process was combined with simultaneous HCD to create a hybrid activation method, UVPD/HCD, with the objective of converting the dead-end charge-reduced electron photodetachment ions into diagnostic product ions. Hybrid activation of biopolymers has provided benefits over individual activation methods in several previous studies of peptides, nucleic acids, and lipids.[41,44,46–48,58,59,74] For example, activated-electron photodetachment (a-EPD), in which UVPD is followed by low energy CID, has been utilized for analysis of lipid A.[41] In an Orbitrap mass spectrometer in which UVPD occurs in the HCD cell at the back end of the instrument, the natural hybrid combination is UVPD with HCD. The resulting hybrid UVPD/HCD spectrum for Kdo_2-lipid A is shown in **Figure 2D**. Compared to UVPD alone, the hybrid UVPD/HCD method resulted in production of fewer ion types, and the significant photodetachment ion observed in **Figure 2C** is absent in **Figure 2D**, presumably converted into other products by the supplemental HCD activation. The most abundant ions observed in the HCD spectrum (**Figure 2B**) are also seen in the hybrid spectrum (**Figure 2D**). Most interestingly, many of the product ions observed in the UVPD spectrum (**Figure 2C**) appear 1 Da lower in mass in the UVPD/HCD spectrum (**Figure 2D**). This outcome is entirely consistent with the fact that these mass-shifted ions likely arise from HCD of the electron photodetachment charge-reduced precursor. In fact, both UVPD and to an even greater extent UVPD/HCD generated a number of fragment ions that exhibited hydrogen migration suggesting that they were generated via a radical mechanism, which has been reported in other UVPD studies of other biopolymers.[41,43–66] Although UVPD/HCD did not provide any new structural information over UPVD, the dissociation efficiency of UVPD/HCD was greater than UVPD alone and the array of observed fragment ions exceeded that of HCD alone, thus providing information about both the lipid A and inner core regions of Kdo_2-Lipid A. One notable difference between CID, HCD, UVPD and UVPD/HCD is the variation in the relative abundances of doubly charged fragment ions. (**Figure S1).** CID, HCD, and UVPD yielded more abundant multiply charged (mostly z = 2−) fragment ions, whereas UVPD/HCD generated more abundant singly charged radical fragment anions. Overall there were notable benefits of UVPD and the hybrid UVPD/HCD method such that they might be utilized in a complementary fashion for LOS analysis. Additional examples of UVPD and UVPD/HCD spectra and their associated fragmentation maps are described in the next section.

LC-MS/MS Characterization of *E. coli* BN1 ΔwaaQwaaG and wild type BN1 LOS

The chromatographic separation of LPS and LOS is a difficult challenge due to inherent solubility issues. The most commonly reported separation methods require hydrolysis or derivatization of LOS but at the cost of removal of informative structural features such as acyl chains or modifications. We recently reported a new method for the LCMS separation of hydrophobic lipid A species in complex mixtures.[70] Briefly, this system utilized a mixed aqueous/organic solvent system to separate individual hydrophobic species prior to MS/MS analysis. The mobile phase was applied as a gradient starting with 50:50 methanol:water and the addition of 0.05% NH_4OH and a 40:40:20 mixture of isopropyl alcohol:chloroform:methanol supplemented with 0.05% NH_4OH for the best solubility, separation and ESI ionization of intact lipids.[66] Here we utilize optimized a similar gradient for separation and analysis of LOS.

LOS were extracted from *E. coli* (strain BN1) with mutations in the WaaQ and WaaG glycosyltransferases (termed BN1 Δ*waaQwaaG*) which prevented the attachment of the outer core hexoses and resulted in incorporation of a single inner core heptose. Deep rough LOS mutants missing their outer core saccharides exhibit higher anti-microbial sensitivity which has been attributed to a decreased outer membrane permeability barrier and poor activity/binding of phosphotransferases.[75] Such LOS truncations impede bacterial fitness through the loss of phosphorylation sites within the LOS/LPS inner core. This prevents neighboring LOS/LPS molecules to properly stabilize and withstand the presence of antimicrobials[76]. For the resulting mixture of LOS, the chromatographic trace, one representative UVPD/HCD mass spectrum, and the corresponding fragmentation map for the predominant LOS are illustrated in **Figure 4**. The survey ESI-mass spectra obtained from profiling the chromatogram of the BN1 Δ*waaQwaaG* mixture revealed the presence of six LOS (**Figure S2)**. The most abundant LOS species is a hexa-acylated lipid A decorated with two Kdo sugars and two heptoses (hexa-acyl *waaQwaaG*). However, analogous penta-acyl and tetra-acyl LOS species eluted just prior to the hexa-acylated waaQwaaG (**Figure 4** and **Figure S2**).

Hexa-acylated *waaQwaaG* was subjected to HCD, UVPD, and HCD/UVPD, and the resulting UVPD and HCD/UVPD mass spectra are displayed in **Figure 4B**. Additional examples of HCD, UVPD and UVPD/HCD mass spectra are provided in **Figures S3 - S12** for the other variations of the *waaQwaaG* LOS (ones containing four to six acyl chains). As expected, based on the far simpler fragmentation pattern afforded by HCD of the Kdo_2-lipid A above, the HCD mass spectrum of the hexa-acylated *waaQwaaG* (**Figure S7**) exhibited prominent cleavages at sites (1), (3) and (5) but did not provide a sufficient number of fragment ions to confidently map the

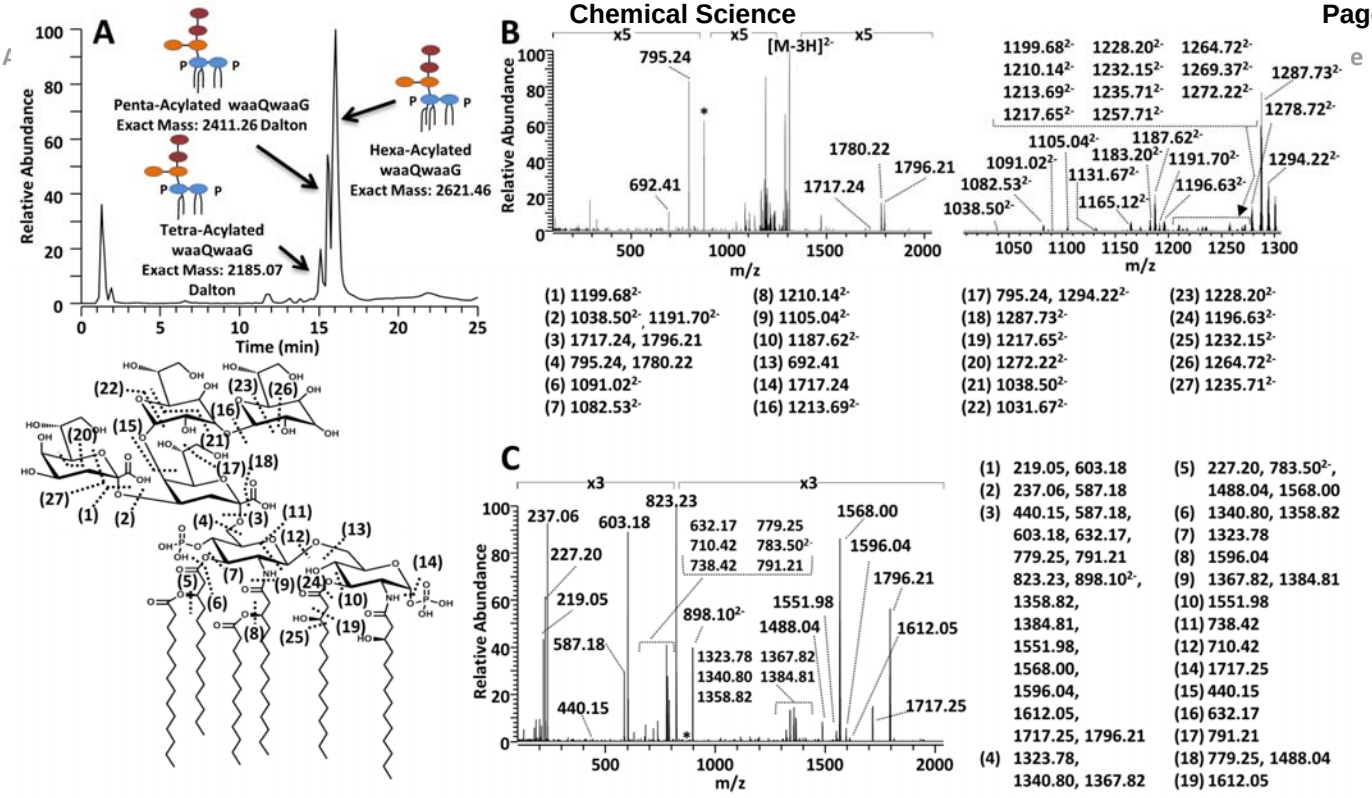

Figure 4. LC-UVPD-MS analysis of lipooligosaccharides from E.coli BN1 ΔwaaQwaaG culture. A) LC-MS trace (top left) of a mixture of LOS from E. coli BN1 ΔwaaQwaaG culture, B) UVPD mass spectrum (top right) and C) UVPD/HCD mass spectrum (lower right) of a hexa-acylated BN1 ΔwaaQwaaG LOS (z = 3—) [Mr = 2621.46]. The zoomed-in region between m/z 1000 and 1300 of the UVPD spectrum is shown on the top right. The fragmentation map of hexa-acylated waaQwaaG LOS is shown the bottom left and the corresponding fragment ions associated with each mass spectrum are shown adjacent to each spectrum.

entire LOS structure. Several serial MS/MS events (MS^n) could be used to provide additional fragmentation information at the cost of diminishing ion signal and difficult implementation on an LCMS time scale.

UVPD of hexa-acylated *waaQwaaG* yielded many informative fragment ions which supported the elucidation of the hydrophilic tetrasaccharide core and the hydrophobic lipid A anchor (**Figure 4B**). In particular the array of glycosidic cleavages (at sites (1), (2), (3), (4), (15) and (16) in **Figure 4B**) allowed the characterization of the inner core structure and a number of C-O, C-N and glucosamine bond cleavages (at sites (5) through (13), (19), (24) and (25)) provided confirmation of the lipid A moiety. UVPD of hexa-acylated waaQwaaG also provided many additional cross-ring glycan cleavages (i.e. cleavages (11), (20) - (23), (26), and (27)) which aided in the elucidation of the complex core branching.

With respect to the hybrid method, UVPD/HCD (**Figure 4C**) provided ample and diverse diagnostic fragments to characterize and identify the LOS structural variation within the BN1 Δ*waaQwaaG* mixture, with greater dissociation efficiency and thus sensitivity than UVPD alone, albeit with none of the cross-ring cleavages unique to UVPD alone. In particular, the fragment ions of *m/z* 1796 (hexaacylation), 1587 (pentaacylation) and 1359 (tetraacylation) in the UVPD/HCD mass spectra (**Figure 4C** and also **Figures S3-S6** for other LOS) provided a direct indication of the number of acyl chains within the intact lipid A anchor of the LOS, while glycosidic and cross ring cleavages within the lipid A anchor ((11) - (13)) allowed the determination of the acylation pattern between the different glucosamine rings arising from the deacylase modifications. A rich array of C-O, C-C and C-N secondary cleavages within the lipid A moiety (cleavages (5) - (10), (19)) in **Figure 4C**) further confirmed the composition of the lipid A acyl chains. Furthermore the UVPD/HCD fragments from cleavage (3) to yield the inner core unit and companion lipid A, respectively) provided a simple and general diagnostic means to identify whether the core glycoform was modified with PPEtN (m/z 1026 as observed in **Figures S5** and **S6**) or without the PPEtN moiety (m/z 823 as observed in **Figure 4** and **Figures S3** and **S4**). Additional glycosidic cleavages within the core sugars ((1) - (3), (15) and (16) in **Figure 4**) occurred upon UVPD/HCD and allowed the characterization of the heptose and Kdo linkages. HCD alone of the same BN1 Δ*waaQwaaG* LOS species (**Figures S7** to **S10**) generally only resulted in cleavage of the linkages between the lipid A and LOS moieties or the Kdo sugars, limiting the characterization of either the hydrophobic or hydrophilic moieties. As noted above, UVPD generated a greater number of cross ring cleavages ((20) - (23), (26) and (27) than UVPD/HCD, as illustrated in **Figure 4** and **Figures S11** to **S12**. It is these cross ring cleavages which are key for characterization the branching patterns of glycans of complex biopolymers.[56,61]

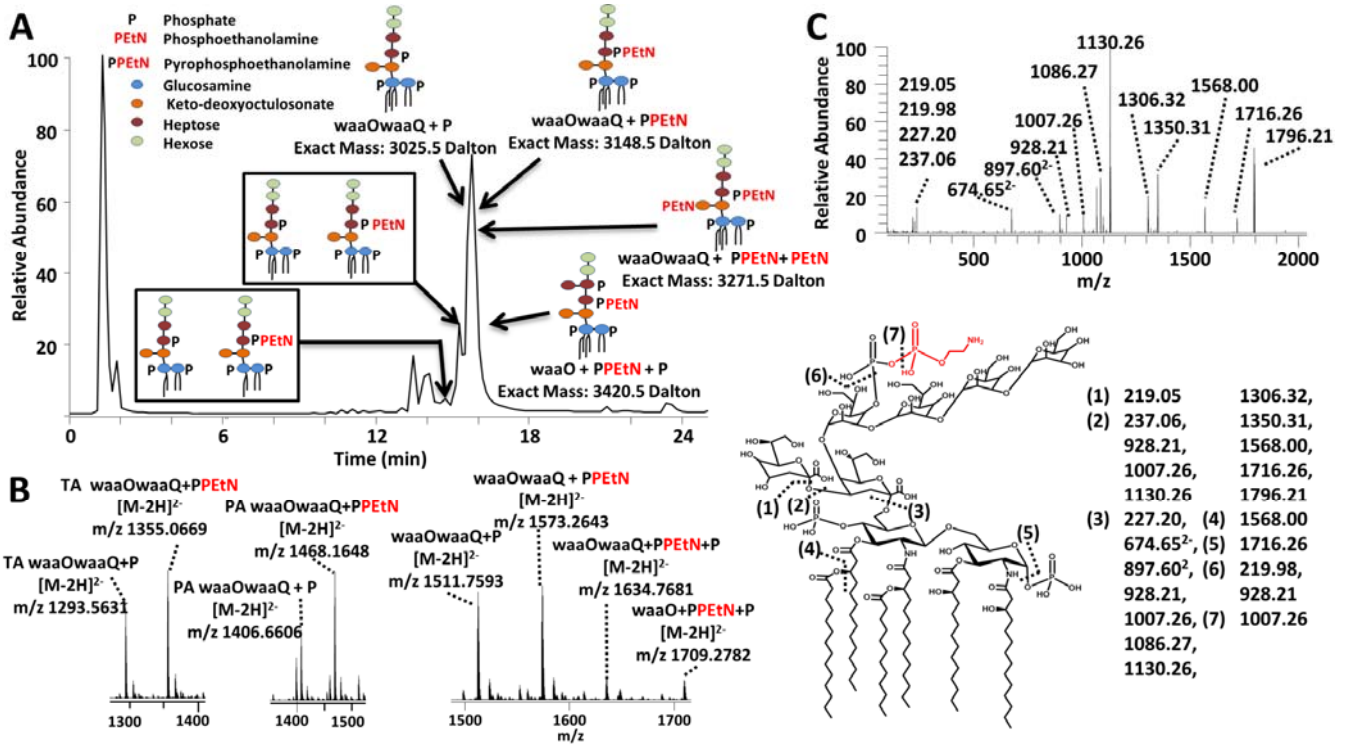

Figure 5. LC-UVPD-MS of lipooligosaccharides from E. coli BN1 culture. A) LC-MS trace of identified E. coli BN1 LOS (top left), and B) survey mass spectra of the identified LOS (bottom left). C) The UVPD/HCD mass spectrum of hexa-acylated waaOwaaQ + PPEtN (3—) [Mr = 3148.5 Da] is shown on the bottom left and the accompanying fragmentation cleavage map is shown on the bottom right. "TA" is an abbreviation for tetra-acyl and "PA" is an abbreviation for penta-acyl.

Mass differences of 203 Da between the dominant molecular ions (z = 2−) observed in the ESI mass spectra of the BN1 Δ*waaQwaaG* LOS (**Figure S2)** suggested that additions of pyrophosphoethanolamine (PPEtN), a modification that is responsible for stabilizing lipid membranes and conferring CAMP resistance, occurred for each of the different LOS cores. The PPEtN modification occurs by a combination of the enzymes waaP (a LOS kinase) and CptA (a phosphoethanolamine (pEtN) transferase). Quantifying the relative amounts of LOS modifications like PPEtN provides insight into cell membrane structural stability which directly impacts bacterial viability and growth. The portion of PPEtN-modified LOS in the LOS obtained from the K12-waaQwaaG strain was calculated (based on integration of peak areas from the extracted ion chromatographic traces) to be 27 ± 1% of the total BN1 Δ*waaQwaaG* LOS. Gram negative bacteria are known to modulate their LOS/LPS acylation patterns to adapt to and resist environmental/antibacterial stresses.[3] The three acylation patterns (tetra, penta, hexa) identified for the BN1 ΔwaaQwaaG LOS sample were quantitated and are summarized in **Table S2** (using the raw peak areas shown in **Table S3**). The tetra-acylated *waaQwaaG* was the least abundant lipid A anchor (15%), followed by the penta-acylated *waaQwaaG* (27%), and the hexa-acylated *waaQwaaG* (58% of the total sample) was the most dominant LOS anchor in the mixture. The variation of PPEtN addition depended to some extent on the acylation pattern of the lipid A anchor. In particular the ratio of PPEtN-modified to unmodified LOS was approximately 0.3:1 for the tetra-acylated and penta-acylated LOS, but it was 0.4:1 for the hexacylated LOS. Quantification of LOS modifications is a difficult analytical task, and the LC-MS method here represents a significant step towards addressing this challenge.

The LC-MS/MS strategy was implemented for evaluation of the LOS extracted from an *E. coli* strain (BN1) which generates wild type K12 LOS. BN1 was produced to strictly generate the highly endotoxic, bis-phosphorylated hexa-acylated lipid A.[8] BN1 provides insight into the wild type *E. coli* core glycosylation patterns and modifications. The resulting LC-MS trace and survey mass spectra of the identified LOS are shown in **Figure 5**. A total of eight unique LOS were identified with mass differences corresponding to variations in either the lipid A acyl chains or the core sugar. HCD/UVPD was used to characterize each LOS, and one representative MS/MS spectrum is shown in **Figure 5c** for waaOwaaQ+PPEtN (a truncated LOS with an inner core containing two Kdo and two heptoses and an outer core with two hexoses) along with its fragmentation map. As described above, cleavage site (3) is a key one because it releases the complementary inner core (m/z 1350.31 for waaOwaaQ-PPEtN) and lipid A (m/z 1796.21) sub-units. Based on the common occurrence of this cleavage site (3) upon UVPD/HCD and formation of the inner core and lipid A sub-units, the lipid A anchors were tracked and identified based on the m/z values of the characteristic lipid A (m/z 1796, m/z 1586 and m/z 1359 for the hexa-acyl, penta-acyl, and tetra-acyl lipid A, respectively, in **Figure S13**). The lipid A moieties were thus determined for each LOS using a combination of the intact masses of the eluting LOS (**Figure 5a** and **b**), their diagnostic UVPD/HCD spectra (for example characteristic fragment ions arising from cleavages (1)-(3) and (6)-(7) in **Figure 5c**), and the known structure of the *E. coli* (K12) core.[77] Three different lipid A acyl chain patterns were observed, including the wild type hexa-acylated lipid A anchor as well as the deacylated penta-acylated and tetra-acylated lipid A which were akin to the same acylation pattern noted for the waaQwaaG LOS in **Figure 4**. Based on the UVPD and

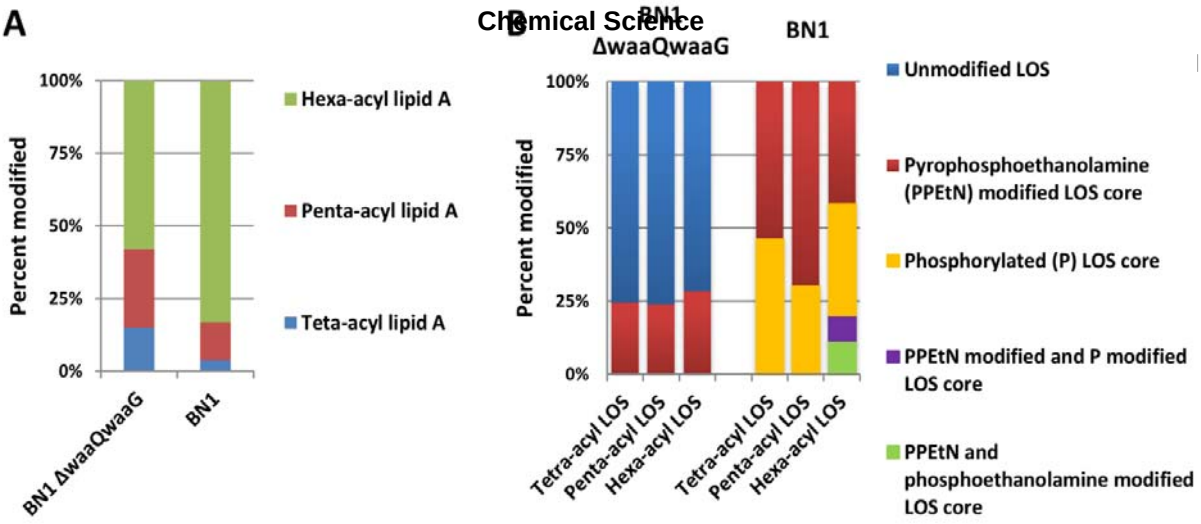

Figure 6. Histograms summarizing (A) the types of lipid A acylation and (B) core modification patterns with respect to acylation pattern for the BN1 and BN1 ΔwaaQwaaG LOS samples. Values were calculated using the results shown in Supplemental Tables S2 and S4.

HCD/UVPD spectra, a total of two LOS glycoforms were identified in the mixture of wild type *E. coli* LOS. Both glycoforms were truncated, with the first containing two Kdo sugars, two heptoses and two hexoses sugars (waaOwaaQ) and the second glycoform similar to the first but with an additional heptose sugar (waaO) attached in the inner core. The LOS identified exhibited a mixture of phosphoethanolamine (+PEtN), pyrophosphoethanolamine (+PPEtN) and phosphate (+P) groups attached to the core sugars. The most predominant core glyco-modifications were additions of phosphates (i.e. waaOwaaQ + P) and pyrophosphoethanolamines (i.e. waaOwaaQ + PPEtN) which were observed for each of the LOS lipid A anchors (tetra, penta and hexa-acylations). Two additional hexa-acylated LOS were discovered with multiple additions of phosphate, phosphoethanolamine and pyrophosphoethanolamine (waaO + PPEtN+ P and waaOwaaQ+PPEtN+PEtN).

An interesting difference in LOS acylation patterns (tetra, penta, hexa) was observed between the BN1 *E. coli* LOS and the further truncated BN1 Δ*waaQwaaG* LOS samples. The wild type BN1sample was most frequently hexa-acylated (84%) (**Figure 6A,** calculated using **Tables S2-S5**), whereas the BN1 Δ*waaQwaaG* sample displayed only 58% hexa-acylated LOS (**Figure 6A**). Furthermore, the types and the total number of modified LOS core sugars differed between the BN1 Δ*waaQwaaG* and BN1 LOS. More specifically the BN1 Δ*waaQwaaG* sample was predominantly unmodified, whereas the BN1 LOS core was consistently modified with either PPEtN or P moieties (**Figure 6B**). Additionally the distribution of LOS core sugars were modified varied depending on the LOS lipid A acylation pattern and the sample type. Specifically 24-28% of the BN1 Δ*waaQwaaG* LOS core was modified with PPEtN (**Figure 6B**), whereas the BN1 LOS samples exhibited a wider PPEtN distribution (ranging from 42 to 70%). This decrease of PPEtN core modification observed in the BN1 Δ*waaQwaaG* likely reflects an increased susceptibility to antimicrobial attack, a known phenotype associated with deep-rough LOS mutants with low phosphorylation.[75] The tetra-acylated BN1 LOS was phosphorylated 46% of the time (**Figure 6B**), whereas the BN1 penta-acyl LOS and BN1 hexa-acyl LOS were modified respectively modified 30% and 38% of the time. Finally the hexa-acyl LOS was the only lipid A acyl pattern with multiple modifications within the core.

Quantification of the LOS core and lipid A structural remodeling provides a new avenue of LOS/LPS characterization. The presented LC-MS method affords the ability to track changing core modifications with respect to lipid A remodeling, which can be observed in the LOS samples. This interplay of core modifications and lipid A acylation patterns in the BN1 and BN1 Δ*waaQwaaG* systems reveals functional and architectural differences of the *E. coli* cell envelope. For example, the BN1 Δ*waaQwaaG* LOS cores were consistently modified regardless of acylation pattern (**Figure 6B**) whereas in the BN1 sample, core modification was biased toward hexa-acylated lipid A (**Figure 6B**). Truncation of the outer core has been associated with decreased core phosphorylation and is known to increase susceptibility to antimicrobial attack,[75,78] which is reflected in the low CptA/WaaP activity (PPEtN addition) in the BN1 Δ*waaQwaaG* LOS sample (**Figure 6**). The BN1 LOS sample on the other hand was observed to have a predominantly completely hexa-acylated lipid A anchor and diverse core modifications, characteristics associated with outer membrane integrity. Although presented here as a proof of concept, this methodology could be further utilized to characterize more complex and global LOS/LPS distributions of the cell membrane. For example, lipid A post-translational modifications enzymes (such as PagP, PagL, LpxR) are known to modulate the cell envelope upon exposure to environmental stresses;[3] however, it is not well known if these modification enzymes target lipid A anchors with specific core and O-antigen domains. Lastly, UVPD is implementable on a large array of mass spectrometer platforms including time-of-flight, ion traps, Orbitraps, and FTICR (Fourier transform ion cyclotron resonance) instrument, thus providing a powerful and far-reaching option for the confident structural elucidation of complex lipids.

Conclusions

UVPD and a new hybrid UVPD/HCD method were employed for the top-down characterization of intact LOS containing both the inner and outer cores. CID and HCD of intact LOS molecules were dominated by glycosidic cleavages, limiting their scope for characterization of either the lipid A or core polysaccharide moieties. UVPD generated the greatest range of fragment ions, including C-O, C-N, C-C throughout the LOS structure, as well as glycosidic and cross-ring cleavages. UVPD-MS outperformed HCD in the sheer variety of types of fragment ions, especially the informative cross-ring cleavages,

but UVPD/HCD provided the best fragment ion sensitivity. An LC-MS/MS strategy was implemented for elucidating differences in intact *E. coli* endotoxin structures, thus revealing the interplay between core stabilizing modifications and the distribution of remodeled lipid A.

Acknowledgements

Funding from the NIH (R01 GM103655 to JSB, AI064184 and AI76322 to MST), Army Research Office (Grant W911NF-12-1-0390 to MST), Cystic Fibrosis Foundation (Grant TRENT13G0 to MST) and the Welch Foundation (F-1155 to JSB) is gratefully acknowledged. We thank Thermo Fisher Scientific with helping on the modifications to the Orbitrap Elite mass spectrometer to allow UVPD.

Notes and references

[a] Department of Chemistry, The University of Texas at Austin, 1 University Station A5300, Austin, TX, USA 78712
[b] The University of Texas at Austin, Department of Molecular Biosciences, 2506 Speedway A5000, Austin, TX, USA 78712.

Electronic Supplementary Information (ESI) available: [details of any supplementary information available should be included here]. See DOI: 10.1039/b000000x/

References

1. M. S. Trent, C. M. Stead, A. X. Tran, and J. V. Hankins, *J. Endotoxin Res.*, 2006, **12**, 205 –223.
2. C. R. H. Raetz, C. M. Reynolds, M. S. Trent, and R. E. Bishop, *Annu. Rev. Biochem.*, 2007, **76**, 295–329.
3. B. D. Needham and M. S. Trent, *Nat. Rev. Microbiol.*, 2013, **11**, 467–481.
4. C. R. H. Raetz and C. Whitfield, *Annu. Rev. Biochem.*, 2002, **71**, 635–700.
5. T. W. Cullen, J. P. O'Brien, D. R. Hendrixson, D. K. Giles, R. I. Hobb, S. A. Thompson, J. S. Brodbelt, and M. S. Trent, *Infect. Immun.*, 2013, **81**, 430 –440.
6. H. Ulm, M. Wilmes, Y. Shai, and H.-G. Sahl, *Front. Immunol.*, 2012, **3**.
7. J. V. Hankins, J. A. Madsen, D. K. Giles, J. S. Brodbelt, and M. S. Trent, *Proc. Natl. Acad. Sci.*, 2012, **109**, 8722–8727.
8. B. D. Needham, S. M. Carroll, D. K. Giles, G. Georgiou, M. Whiteley, and M. S. Trent, *Proc. Natl. Acad. Sci.*, 2013, **110**, 1464–1469.
9. L. M. Bogomolnaya, C. A. Santiviago, H.-J. Yang, A. J. Baumler, and H. L. Andrews-Polymenis, *Mol. Microbiol.*, 2008, **70**, 1105–1119.
10. M. L. Kim and J. M. Slauch, *FEMS Immunol. Med. Microbiol.*, 1999, **26**, 83–92.
11. T. C. Meredith, U. Mamat, Z. Kaczynski, B. Lindner, O. Holst, and R. W. Woodard, *J. Biol. Chem.*, 2007, **282**, 7790–7798.
12. S. Gulati, A. Cox, L. A. Lewis, F. S. Michael, J. Li, R. Boden, S. Ram, and P. A. Rice, *Infect. Immun.*, 2005, **73**, 7390–7397.
13. M. Muse, C. Grandjean, T. K. Wade, and W. F. Wade, *FEMS Immunol. Med. Microbiol.*, 2012, **66**, 98–115.
14. H. Kojima, M. Inagaki, T. Tomita, and T. Watanabe, *Rapid Commun. Mass Spectrom.*, 2010, **24**, 43–48.
15. A. Silipo, S. Leone, A. Molinaro, L. Sturiale, D. Garozzo, E. L. Nazarenko, R. P. Gorshkova, E. P. Ivanova, R. Lanzetta, and M. Parrilli, *Eur. J. Org. Chem.*, 2005, **2005**, 2281–2291.
16. L. Sturiale, D. Garozzo, A. Silipo, R. Lanzetta, M. Parrilli, and A. Molinaro, *Rapid Commun. Mass Spectrom.*, 2005, **19**, 1829–1834.
17. A. Kilár, Á. Dörnyei, A. Bui, Z. Szabó, B. Kocsis, and F. Kilár, *J. Mass Spectrom.*, 2011, **46**, 61–70.
18. H. Therisod, V. Labas, and M. Caroff, *Anal. Chem.*, 2001, **73**, 3804–3807.
19. M. M. Corsaro, G. Pieretti, B. Lindner, R. Lanzetta, E. Parrilli, M. L. Tutino, and M. Parrilli, *Chem. – Eur. J.*, 2008, **14**, 9368–9376.
20. A. Hanuszkiewicz, G. Hübner, E. Vinogradov, B. Lindner, L. Brade, H. Brade, J. Debarry, H. Heine, and O. Holst, *Chem. – Eur. J.*, 2008, **14**, 10251–10258.
21. U. Zähringer, B. Lindner, Y. A. Knirel, W. M. R. van den Akker, R. Hiestand, H. Heine, and C. Dehio, *J. Biol. Chem.*, 2004, **279**, 21046–21054.
22. J. Li, R. W. Purves, and J. C. Richards, *Anal Chem*, 2004, **76**, 4676–4683.
23. A. C. Casabuono, C. A. van der Ploeg, A. D. Rogé, S. B. Bruno, and A. S. Couto, *Rapid Commun. Mass Spectrom.*, 2012, **26**, 2011–2020.
24. S. Ummarino, M. M. Corsaro, R. Lanzetta, M. Parrilli, and J. Peter-Katalinic, *Rapid Commun. Mass Spectrom.*, 2003, **17**, 2226–2232.
25. J. Lukasiewicz, W. Jachymek, T. Niedziela, L. Kenne, and C. Lugowski, *J. Lipid Res.*, 2010, **51**, 564–574.
26. A. Silipo, C. De Castro, R. Lanzetta, A. Molinaro, M. Parrilli, G. Vago, L. Sturiale, A. Messina, and D. Garozzo, *J. Mass Spectrom.*, 2008, **43**, 478–484.
27. B. Schilling, M. K. McLendon, N. J. Phillips, M. A. Apicella, and B. W. Gibson, *Anal Chem*, 2007, **79**, 1034–1042.
28. J. W. Jones, I. E. Cohen, F. Tureček, D. R. Goodlett, and R. K. Ernst, *J. Am. Soc. Mass Spectrom.*, 2010, **21**, 785–799.
29. J. W. Jones, S. A. Shaffer, R. K. Ernst, D. R. Goodlett, and F. Tureček, *Proc. Natl. Acad. Sci.*, 2008, **105**, 12742–12747.
30. Y. S. Ting, S. A. Shaffer, J. W. Jones, W. V. Ng, R. K. Ernst, and D. R. Goodlett, *J. Am. Soc. Mass Spectrom.*, 2011, **22**, 856–866.
31. I. Mikhail, H. H. Yildirim, E. C. H. Lindahl, and E. K. H. Schweda, *Anal. Biochem.*, 2005, **340**, 303–316.
32. S. H. Yoon, Y. Huang, J. S. Edgar, Y. S. Ting, S. R. Heron, Y. Kao, Y. Li, C. D. Masselon, R. K. Ernst, and D. R. Goodlett, *Anal. Chem.*, 2012, **84**, 6530–6537.
33. S. A. Shaffer, M. D. Harvey, D. R. Goodlett, and R. K. Ernst, *J. Am. Soc. Mass Spectrom.*, 2007, **18**, 1080–1092.
34. A. El-Aneed and J. Banoub, *Rapid Commun. Mass Spectrom.*, 2005, **19**, 1683–1695.
35. G. Madalinski, F. Fournier, F.-L. Wind, C. Afonso, and J.-C. Tabet, *Int. J. Mass Spectrom.*, 2006, **249–250**, 77–92.
36. S. M. Boué and R. B. Cole, *J. Mass Spectrom.*, 2000, **35**, 361–368.
37. A. Kussak and A. Weintraub, *Anal. Biochem.*, 2002, **307**, 131–137.
38. S. Chan and V. N. Reinhold, *Anal. Biochem.*, 1994, **218**, 63–73.
39. M. R. Pelletier, L. G. Casella, J. W. Jones, M. D. Adams, D. V. Zurawski, K. R. O. Hazlett, Y. Doi, and R. K. Ernst, *Antimicrob. Agents Chemother.*, 2013, **57**, 4831–4840.
40. D. M. B. Post, L. Yu, B. C. Krasity, B. Choudhury, M. J. Mandel, C. A. Brennan, E. G. Ruby, M. J. McFall-Ngai, B. W. Gibson, and M. A. Apicella, *J. Biol. Chem.*, 2012, **287**, 8515–8530.

41. J. A. Madsen, T. W. Cullen, M. S. Trent, and J. S. Brodbelt, *Anal Chem*, 2011, **83**, 5107–5113.
42. A. Kilár, Á. Dörnyei, and B. Kocsis, *Mass Spectrom. Rev.*, 2013, **32**, 90–117.
43. J. S. Brodbelt, *J. Am. Soc. Mass Spectrom.*, 2011, **22**, 197–206.
44. J. A. Madsen, R. R. Cheng, T. S. Kaoud, K. N. Dalby, D. E. Makarov, and J. S. Brodbelt, *Chem. - Eur. J.*, 2012, **18**, 5374–5383.
45. J. P. Reilly, *Mass Spectrom. Rev.*, 2009, **28**, 425–447.
46. S. I. Smith and J. S. Brodbelt, *Anal Chem*, 2010, **83**, 303–310.
47. S. I. Smith and J. S. Brodbelt, *Anal Chem*, 2010, **82**, 7218–7226.
48. V. Gabelica, F. Rosu, E. Pauw, R. Antoine, T. Tabarin, M. Broyer, and P. Dugourd, *J. Am. Soc. Mass Spectrom.*, 2007, **18**, 1990–2000.
49. F. Rosu, V. Gabelica, E. De Pauw, R. Antoine, M. Broyer, and P. Dugourd, *J Phys Chem A*, 2012, **116**, 5383–5391.
50. T. Ly and R. R. Julian, *Angew. Chem. Int. Ed.*, 2009, **48**, 7130–7137.
51. S. H. Yoon, J. H. Moon, and M. S. Kim, *J. Mass Spectrom.*, 2010, **45**, 806–814.
52. J. W. Morgan and D. H. Russell, *J. Am. Soc. Mass Spectrom.*, 2006, **17**, 721–729.
53. Z. Guan, N. L. Kelleher, P. B. O'Connor, D. J. Aaserud, D. P. Little, and F. W. McLafferty, *Int. J. Mass Spectrom. Ion Process.*, 1996, **157–158**, 357–364.
54. Q. Enjalbert, M. Girod, R. Simon, J. Jeudy, F. Chirot, A. Salvador, R. Antoine, P. Dugourd, and J. Lemoine, *Anal. Bioanal. Chem.*, 2013, **405**, 2321–2331.
55. J. K. Diedrich and R. R. Julian, *Anal Chem*, 2010, **82**, 4006–4014.
56. B. J. Ko and J. S. Brodbelt, *Anal. Chem.*, 2011, **83**, 8192–8200.
57. A. Racaud, R. Antoine, P. Dugourd, and J. Lemoine, *J. Am. Soc. Mass Spectrom.*, 2010, **21**, 2077–2084.
58. H. T. Pham, T. Ly, A. J. Trevitt, T. W. Mitchell, and S. J. Blanksby, *Anal. Chem.*, 2012, **84**, 7525–7532.
59. H. T. Pham, A. J. Trevitt, T. W. Mitchell, and S. J. Blanksby, *Rapid Commun. Mass Spectrom.*, 2013, **27**, 805–815.
60. A. Devakumar, D. K. O'Dell, J. M. Walker, and J. P. Reilly, *J. Am. Soc. Mass Spectrom.*, 2008, **19**, 14–26.
61. J. P. O'Brien and J. S. Brodbelt, *Anal. Chem.*, 2013, **85**, 10399–10407.
62. J. V. Hankins, J. A. Madsen, D. K. Giles, J. S. Brodbelt, and M. S. Trent, *Proc. Natl. Acad. Sci.*, 2012.
63. J. V. Hankins, J. A. Madsen, B. D. Needham, J. S. Brodbelt, and M. S. Trent, in *Bacterial Cell Surfaces*, ed. A. H. Delcour, Humana Press, Totowa, NJ, 2013, vol. 966, pp. 239–258.
64. J. C. Henderson, J. P. O'Brien, J. S. Brodbelt, and M. S. Trent, *J. Vis. Exp.*, 2013, e50623.
65. J. V. Hankins, J. A. Madsen, D. K. Giles, B. M. Childers, K. E. Klose, J. S. Brodbelt, and M. S. Trent, *Mol. Microbiol.*, 2011, **81**, 1313–1329.
66. J. P. O'Brien, B. D. Needham, J. C. Henderson, E. M. Nowicki, M. S. Trent, and J. S. Brodbelt, *Anal. Chem.*, 2014.
67. H. Kojima, M. Inagaki, T. Tomita, T. Watanabe, and S. Uchida, *J. Chromatogr. B*, 2009, **877**, 1537–1542.
68. S. L. Lundstrom, J. Li, M. Mansson, M. Figueira, M. Leroy, R. Goldstein, D. W. Hood, E. R. Moxon, J. C. Richards, and E. K. H. Schweda, *Infect. Immun.*, 2008, **76**, 3255–3267.
69. H. Kojima, M. Inagaki, T. Tomita, T. Watanabe, and S. Uchida, *J. Chromatogr. B*, 2010, **878**, 442–448.
70. J. Smit, I. A. Kaltashov, R. J. Cotter, E. Vinogradov, M. B. Perry, H. Haider, and N. Qureshi, *Innate Immun.*, 2008, **14**, 25–36.
71. T. F. Kalhorn, A. Kiavand, I. E. Cohen, A. K. Nelson, and R. K. Ernst, *Rapid Commun. Mass Spectrom.*, 2009, **23**, 433–442.
72. J. B. Shaw, W. Li, D. D. Holden, Y. Zhang, J. Griep-Raming, R. T. Fellers, B. P. Early, P. M. Thomas, N. L. Kelleher, and J. S. Brodbelt, *J. Am. Chem. Soc.*, 2013, **135**, 12646–12651.
73. C. R. H. Raetz, T. A. Garrett, C. M. Reynolds, W. A. Shaw, J. D. Moore, D. C. Smith, A. A. Ribeiro, R. C. Murphy, R. J. Ulevitch, C. Fearns, D. Reichart, C. K. Glass, C. Benner, S. Subramaniam, R. Harkewicz, R. C. Bowers-Gentry, M. W. Buczynski, J. A. Cooper, R. A. Deems, and E. A. Dennis, *J. Lipid Res.*, 2006, **47**, 1097–1111.
74. C. K. Frese, A. F. M. Altelaar, H. van den Toorn, D. Nolting, J. Griep-Raming, A. J. R. Heck, and S. Mohammed, *Anal. Chem.*, 2012, **84**, 9668–9673.
75. J. A. Yethon, E. Vinogradov, M. B. Perry, and C. Whitfield, *J. Bacteriol.*, 2000, **182**, 5620–5623.
76. E. Frirdich and C. Whitfield, *J. Endotoxin Res.*, 2005, **11**, 133–144.
77. E. Frirdich, B. Lindner, O. Holst, and C. Whitfield, *J. Bacteriol.*, 2003, **185**, 1659–1671.
78. C. Viau, V. Le Sage, D. K. Ting, J. Gross, and H. Le Moual, *J. Bacteriol.*, 2011, **193**, 2168–2176.

